Transport model for homogenized uniaxial wire media: Three-dimensional scattering problems and homogenized model limits

Ebrahim Forati and George W. Hanson*

Department of Electrical Engineering, University of Wisconsin Milwaukee, Milwaukee, Wisconsin 53211, USA

(Received 28 February 2013; revised manuscript received 26 July 2013; published 16 September 2013)

A transport-based formulation is used to model three-dimensional objects made of a uniaxial wire medium. The resulting drift-diffusion equation is used to calculate the extinction/scattering cross section of various uniaxial wire medium objects. A comparison is made with measurement and full wave simulation results. This method is faster than full wave simulation and provides physical insight into electrodynamic processes within the homogenized medium. The effect of wire period and thickness on the homogenized model is investigated, and a Debye length parameter is used to access the effect of wire length.

DOI: 10.1103/PhysRevB.88.125125 PACS number(s): 41.20.Jb, 52.25.Os, 52.40.Db, 84.40.−x

I. INTRODUCTION

Wire media, which form an artificial plasma, have been known since the 1960s.[1,2] However, the interest in wire media was renewed in 2000–2001[3] and studies have shown the importance of spatial dispersion in wire medium models.[4–6] Since then many interesting applications have been reported, such as in superlensing and subwavelength imaging,[7–18] cloaking,[19] shielding,[20] and antennas.[21,22] Wire media are the only known bulk metamaterials without resonant dispersion and losses.[23] Several methods have been introduced for modeling the wire medium at a level of analysis beyond the simple local plasma idea.[24–27] For example, in Ref. 26 an analytical method was proposed to calculate the band structure of a wire mesh crystal. For an unbounded periodic wire medium Floquet analysis can be applied for wave propagation problems. In the case that the period of the wires is much smaller than the wavelength, the fundamental Floquet mode can explain wave propagation in the medium. In this case the wire medium can be homogenized, which is essential for the theory of artificial media. This approximation, along with several other approximations and mathematical techniques, was considered in Ref. 27.

Recently, several works have reported on scattering from finite-sized arrays of wires.[28–31] In this work, we use the drift-diffusion model introduced in Ref. 27 to solve scattering problems involving three-dimensional objects made of a uniaxial wire medium. First, we review the conventional formulation of local and nonlocal scattering problems. Then we use the drift-diffusion model to find the extinction/scattering cross section of a wire medium cube. We also use a commercial full wave package,[32] validated by measurement, for comparison to the drift-diffusion result. In the last section, using the transport model and relating it to physical plasma concepts, we investigate requirements for size of the object, wire period, and wire thickness in order that the homogenization is valid. In the following we consider nonmagnetic uniaxial wire media and the time convention (suppressed) is $e^{j\omega t}$.

II. DIRECT INTEGRAL EQUATION METHOD FOR HOMOGENIZED NONLOCAL MATERIALS

The interaction of a wire medium and an electromagnetic wave has been studied in a few papers by modeling the wire medium in finite difference time domain (FDTD)[33–35] and using commercial simulation codes.[36] In this work we show for a uniaxial wire medium that the drift-diffusion approach provides an accurate model that captures the relevant physics. We will start first with the usual local case, and then describe the extension to nonlocal materials.

The usual method of solving a local scattering problem is to replace the object having complex permittivity tensor $\underline{\varepsilon}$ with equivalent polarization currents and to use Ohm's law in the space domain, leading to an integral equation such as[37]

$$\mathbf{J}(\mathbf{r}) = \underline{\sigma}(\mathbf{r}) \cdot [\mathbf{E}^{\text{sca}}(\mathbf{r}) + \mathbf{E}^{\text{inc}}(\mathbf{r})] \tag{1}$$

for all $\mathbf{r} \subset \Omega$, with Ω being the domain of the object, $\mathbf{J}(\mathbf{r})$ the total polarization current, and $\underline{\sigma}(\mathbf{r})$ the equivalent conductivity which is a function of position, $\underline{\sigma}(\mathbf{r}) = j\omega(\underline{\varepsilon} - \varepsilon_0)$, where ε_0 is the background permittivity. Also, $\mathbf{E}^{\text{inc}}$ is the incident field, $\mathbf{E}^{\text{sca}}$ is the scattered field,

$$\mathbf{E}^{\text{sca}}(\mathbf{r}) = -j\omega\mu \int \underline{\mathbf{G}}_{\text{ee}}(\mathbf{r},\mathbf{r}') \cdot \mathbf{J}(\mathbf{r}')d\Omega', \tag{2}$$

and $\underline{\mathbf{G}}_{\text{ee}}(\mathbf{r},\mathbf{r}')$ is the electric dyadic Green's function for an unbounded medium.

However, if the material is nonlocal, Ohm's law becomes[38]

$$\mathbf{J}(\mathbf{r}) = \int \underline{\sigma}(\mathbf{r},\mathbf{r}') \cdot [\mathbf{E}^{\text{inc}}(\mathbf{r}') + \mathbf{E}^{\text{sca}}(\mathbf{r}')]d\Omega', \tag{3}$$

where, for a translationally invariant medium, $\underline{\sigma}(\mathbf{r},\mathbf{r}') = \underline{\sigma}(\mathbf{r} - \mathbf{r}')$, such that Eq. (3) will be a convolution integral. We use the bulk (translationally invariant) material parameters up to the material boundary; enforcing the additional boundary condition as described below appropriately accounts for the material termination.[39]

Therefore, in the nonlocal case, Eqs. (2) in Eq. (3) results in an at least six-fold integral equation. For a wire medium, $\underline{\sigma}(\mathbf{r} - \mathbf{r}')$ also involves differentiation operators which add more complexity to the formulation. As an example, the equivalent permittivity (and therefore the equivalent conductivity) of an isotropic connected wire medium in space domain involves a second derivative operator[40]

$$\frac{\underline{\varepsilon}(\mathbf{r})}{\varepsilon_0} = (\varepsilon_h - \kappa)\,\delta(\mathbf{r})\,\underline{\mathbf{I}} - \kappa\nabla\nabla\frac{e^{-j\alpha r}}{4\pi r}, \tag{4}$$

where $\delta(\mathbf{r})$ is the Dirac delta function, and κ and α are functions of wire medium parameters as defined by the authors of Refs. 41 and 42.

The permittivity tensor of a uniaxial wire medium has a similar complexity. As a result, in what might be called the direct integral equation method since it results from the basic definition of nonlocal response, solving three-dimensional nonlocal scattering problems is an intense and computationally expensive numerical process, and may as a practical matter be nearly impossible (e.g., solving six-fold or higher integral equations).

III. TRANSPORT APPROACH FOR UNIAXIAL WIRE MEDIUM

As a solution to the issues described in the previous section, we use the transport model introduced by the authors of Refs. 42 and 43. Based on this model, for a wire medium (see, e.g., the insert of Fig. 1) we can form a drift-diffusion equation that relates homogenized conduction current, electric field, and conduction charge density as

$$\mathbf{J_c}(\mathbf{r}) = \underline{\sigma} \cdot \mathbf{E}(\mathbf{r}) - \underline{\mathbf{D}} \cdot \nabla \rho_c(\mathbf{r}) \tag{5}$$

in which $\underline{\sigma}$ is the (local) conductivity tensor and $\underline{\mathbf{D}}$ is the diffusion tensor. For the drift-diffusion model the equivalent conductivity and diffusion parameters are[42]

$$\sigma_{zz} = j\omega\varepsilon_0 \left(\frac{1}{(\varepsilon_m - \varepsilon_h) f_V} - \frac{\omega^2}{\beta_p^2 c^2} \right)^{-1}, \tag{6}$$

$$D_{zz} = j\omega \left[\left(\frac{\varepsilon_h \beta_p^2}{(\varepsilon_m - \varepsilon_h) f_V} - \frac{\varepsilon_h \omega^2}{c^2} \right) \right]^{-1}, \tag{7}$$

where for a uniaxial wire medium with wires parallel to the z axis the other tensor components are zero. In the above expressions, ε_m is the permittivity of the wires, c is the speed of light, ε_h is the permittivity of the host medium, f_V is the volume fraction of wires ($f_V = \pi d^2/4p^2$, where d is the wire diameter and p is the wire period), and β_p is the plasma wave

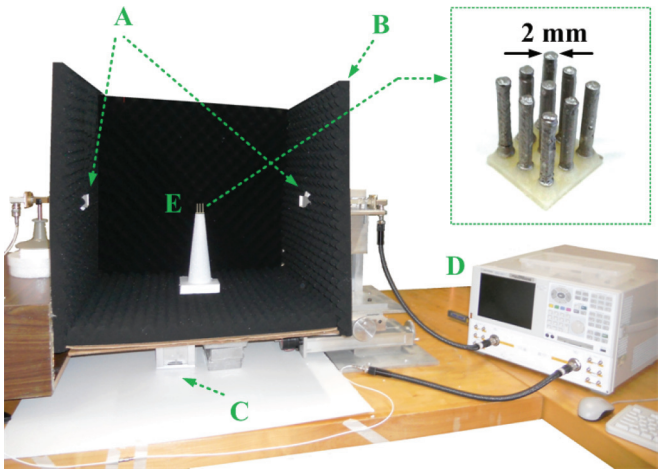

FIG. 1. (Color online) Measurement setup. A: x-band horn antennas, B: microwave absorbers, C: height adjustment, D: E8361A Network analyzer, E: a fabricated 3 × 3 wire object on a styrofoam pedestal. The insert shows a fabricated wire medium with a plastic substrate support. Wire diameter, period, and length are 2, 4, and 12 mm, respectively.

number[27]

$$\beta_p = \omega_p \sqrt{\mu_0 \varepsilon_0} \simeq \frac{1}{p} \sqrt{\frac{2\pi}{ln\left(\frac{p}{\pi d}\right) + 0.5275}}. \tag{8}$$

Diffusion can be "turned off" by setting $\underline{\mathbf{D}} = \underline{\mathbf{0}}$, in which case Eq. (5) leads to the local Ohm's law.

Assuming that the host medium of the wires is the same as the background there is no polarization response, in which case using Eq. (5), Maxwell's equations, and the continuity equation, we obtain the integral equation (IE)

$$\left(1 - \frac{D}{j\omega} \frac{d^2}{dz^2}\right) J_z(\mathbf{r}) = \sigma E_z^{\text{inc}}(\mathbf{r}) - \sigma j\omega\mu \int G_{ee}^{zz}(\mathbf{r},\mathbf{r}') J_z(\mathbf{r}') d\Omega', \tag{9}$$

where G_{ee}^{zz} is the zz component of the electric field dyadic Green's function.[44]

This integrodifferential equation can be solved numerically by expanding J_z in terms of a set of complete basis functions for the given geometry. We also need to enforce the following additional boundary condition (ABC),[45]

$$\mathbf{J} \cdot \hat{\mathbf{n}} = 0, \tag{10}$$

where $\hat{\mathbf{n}}$ is the outward unit vector normal to the surface of the object. It is clear that solving Eq. (9) is much easier than solving Eq. (3). In all of the examples in this paper we assume rectangular objects with the dimensions of a, a, and b in x, y, and z, respectively, and the incident wave is assumed to propagate in the y direction with its electric field either parallel or perpendicular to the wires.

To solve Eq. (9) using the collocation method, we expand $J_z(x,y,z)$ as

$$J_z(x,y,z) = \sum_{m=1}^{M} \sum_{n=1}^{N} \sum_{k=1}^{K} P_{mn}(x,y) \times \left[C_{mnk} \sin\left(k\frac{\pi}{b}z\right) + D_{mnk} \cos\left(k\frac{\pi}{b}z\right) \right] \tag{11}$$

in which

$$P_{mn}(x,y) = \begin{cases} 1 & \frac{(m-1)a}{M} \leqslant x < \frac{ma}{M}, \ \frac{(n-1)a}{N} \leqslant y < \frac{na}{N} \\ 0 & \text{otherwise} \end{cases} \tag{12}$$

are pulse functions; M, N, and K are the number of expansion functions in the in x, y, and z directions, respectively; and C_{mnk} and D_{mnk} are unknown coefficients of the expansion. The ABC (10) should be enforced at the $z = 0$ and $z = b$ planes.

After finding the equivalent currents for the object, we can use the optical theorem to calculate the extinction cross section

$$\sigma^{\text{ext}} = \frac{4\pi}{k^2} \text{Im}\left(\frac{kr}{E_0 e^{jkr}} \mathbf{E}_s^{\parallel} \right), \tag{13}$$

in which $\mathbf{E}_s^{\parallel}$ is the far scattered field in the forward direction copolarized with the incident field. In Ref. 46, the optical theorem is proved for objects consisting of local materials, but it is easy to repeat the same derivation for nonlocal materials.

The extinction cross section is equal to the scattering cross section in our examples since objects are considered lossless.

A rapid prototyping machine (dimension Elite 3D Printer) was used to fabricate wire medium objects out of P430 AB-Splus, which is a plastic material with $\varepsilon_r = 2.53$ [measured in our laboratory at 2.7 GHz using a split post dielectric resonator (SPDR)[47]]. After the wires are formed, they are coated with silver paint[48] to form conducting wires. This process results in a several-micron-thick conductive layer on the insulating "wire" support, so we can consider the resulting wires as perfectly conducting at microwave frequencies. In the insert of Fig. 1 an example of a fabricated wire medium object is shown. At the frequencies considered the object in Fig. 1 forms a cube of homogenized wire medium consisting of a three-wire by three-wire array with wire diameter $d = 2$ mm, wire period $p = 4$ mm, and wire length 12 mm. To make the wires self supporting, they are connected together at one end by a 1-mm thick plastic substrate. Although the scattered cross section of the substrate is small, it causes a frequency shift in the scattered field compared to the ideal wire medium without the substrate. The drift-diffusion IE could be coupled to an IE for the polarization response of the plastic substrate, but here we avoid this complication to concentrate on the wire medium itself. Therefore, we first simulate the exact fabricated object (with the substrate) in CST and compare its results with measurement. After confirming the accuracy of the CST results, we use CST without the substrate to validate the drift-diffusion method.

The setup for the measurements consisted of an anechoic box, two x-band horns and an E8361A Agilent network analyzer (Fig. 1). A Styrofoam pedestal is used to support the wire object. After measuring the forward scattered field, the optical theorem (13) is used to find the extinction cross section. A 3.81-cm diameter brass sphere is used for calibration. Since we are using x-band horn antennas, measurements can be performed in the 7–14-GHz frequency range. This measurement scheme was used by the authors of Ref. 43 to measure the cross section of connected wire medium spheres.

Figure 2 shows the normalized scattering cross section of the 3×3 wire object with substrate, for electric field

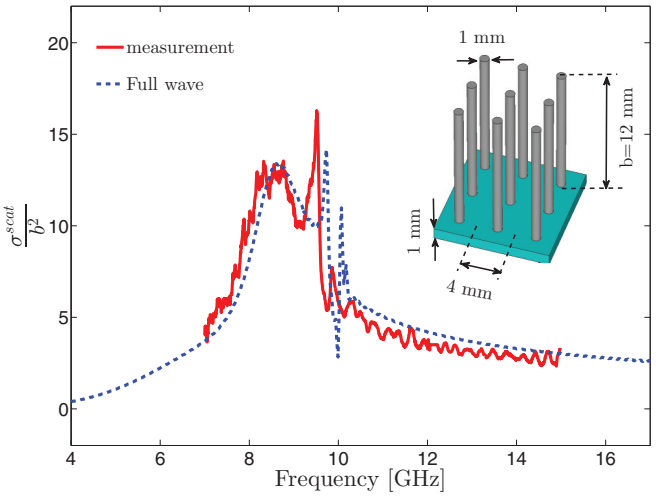

FIG. 2. (Color online) Normalized scattering cross section of a 3×3 wire cubical object with a 1-mm substrate. The incident electric field and wires are parallel.

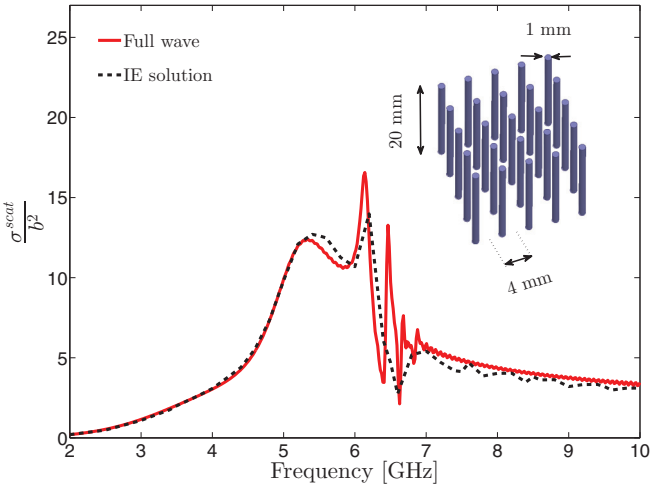

FIG. 3. (Color online) Normalized scattering cross section of a 5×5 wire cubical object.

polarization parallel to the wires. The good agreement between the full wave (CST) and measured results show the validity of the full wave simulation, which will be used for comparison to the drift-diffusion results in the remainder of the paper. Figure 3 shows the normalized cross section of a 5×5 wire cubical object without the substrate. For the drift-diffusion IE, Eqs. (9) and (11) are used with $M = 3$, $N = 4$, $K = 3$. The wire period, diameter, and length are 4, 1, and 20 mm, respectively. These parameters are chosen so that the homogenization approximations leading to the transport model are valid in the chosen frequency interval. It is evident from Fig. 3 that the drift-diffusion method is in good agreement with the full wave results. By comparing the full wave results in Figs. 2 and 3, a frequency shift of more than 1 GHz caused by the substrate is evident.

IV. DEBYE LENGTH AND HOMOGENIZATION PARAMETERS

Having established the transport model, we can take the opportunity afforded by having a three-dimensional simulation to access how the wire parameters affect the validity of the homogenization. In deriving the homogenized results in Ref. 27, which lead to Eqs. (6) and (7) without further approximation, the following assumptions were made: (1) the wire diameter is much smaller than the period, $d \ll p$, (2) $|\mathbf{q}|p \ll 2\pi$, where $\mathbf{q}$ is the electromagnetic wave vector such that $p \ll \lambda$ in the medium, (3) the wires are infinitely long, and (4) the medium is periodic. In this section we consider these aspects. Using the transport model, in Ref. 42 the Debye length of an artificial plasma formed by a wire medium is shown to be

$$\lambda_D = 2\pi\left(\frac{\sigma + j\omega\varepsilon}{D\varepsilon}\right)^{-\frac{1}{2}} \simeq \frac{2\pi}{\beta_p}\sqrt{\frac{\varepsilon_r}{\varepsilon_h}} = \lambda_p\sqrt{\frac{\varepsilon_r}{\varepsilon_h}}$$
$$= p\sqrt{2\pi\left[\ln\left(\frac{p}{\pi d}\right) + 0.5275\right]}\sqrt{\frac{\varepsilon_r}{\varepsilon_h}}, \qquad (14)$$

where in this case the Debye length is defined along the wires. The Debye length is weakly frequency dependent well below

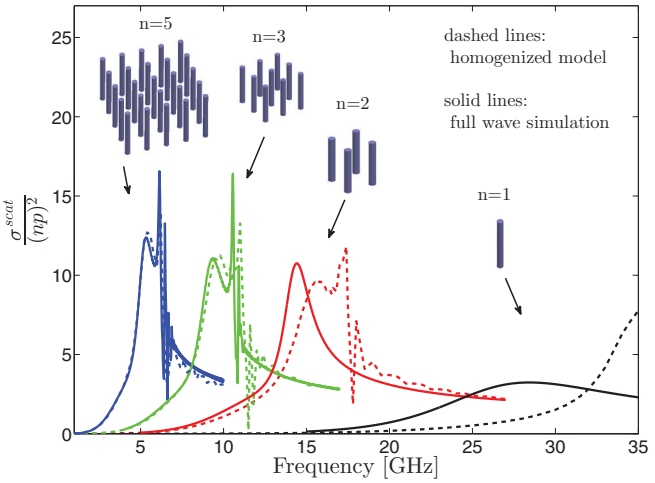

FIG. 4. (Color online) Normalized scattering cross section of cubical objects with different number of wires. Wires have $p = 4$ mm and $d = 1$ mm.

the plasma frequency, and is primarily dependent on the wire parameters; it is strongly dependent on period and weakly dependent on wire diameter, as shown in Eq. (14). Assuming $\varepsilon_r \sim \varepsilon_h$, then if $p \gtrsim \pi d$ (which should be the case per the assumption above), $\lambda_D \gtrsim p$.

The Debye length can be used to find the minimum size of a wire medium object that can be modeled using homogenization. The criteria that the Debye length be small compared to the physical size of the plasma (quasineutrality condition) is often taken as a basic condition for a system to behave as a plasma. For a wire medium we have a similar situation—if wire length b is less than the Debye length then the current induced on the wire will differ considerably from the case of a longer wire. This will lead to a per-unit-length polarizability that, for $b < \lambda_D$, differs from the infinite-wire case, violating a basic assumption of the homogenization. Accordingly, in order that a wire medium can be considered to be an artificial plasma, wires should be longer than the Debye length, which is, itself, typically larger then the wire period (and becomes increasingly larger than the period as period increases). For example, $d = 1$ mm and $p = 4$ mm, the Debye length is approximately 9 mm in the 1–15 GHz frequency interval. Therefore, in this case the object should be larger than 9 mm to have a meaningful artificial plasma. Moreover, the object should accommodate enough wires within itself so that the fundamental Floquet mode suffices for the homogenization. As an illustration of these two requirements, assumptions 3 and 4, cubical objects with sizes of 4, 8, 12, and 20 mm (which accommodate 1, 2, 3, and 5 wires, respectively) are considered in Fig. 4 for $p = 4$ mm, and $d = 1$ mm. As wires are added the wire length was increased so that the objects remained cubical, hence the resonances shift to lower frequencies. As expected, for a single wire the homogenized model is not a good approximation since the object size is smaller than the Debye length and also the object is not periodic. However, even for a 2×2 wire array, having size $8 \times 8 \times 8$ mm, the object is larger than the Debye length and the homogenized model applies to a fairly good approximation, still there is a large frequency shift between the results. Obviously, as the number of wires in the object increases, the homogenized model becomes more accurate. Further, measurements confirm that for a 5×5 wire object with period 4 mm, homogenization becomes increasingly inaccurate as wire length is reduced below the Debye length as shown in Fig. 5. For $b \simeq \lambda_D$, the frequency shift (of the peak in the curves) is about 1 GHz. For $b \simeq 1.5\lambda_D$ and $b \simeq 2\lambda_D$, the shift is 300 MHz, and less than 100 MHz, respectively.

The homogenization used to derive Eqs. (7) and (6) is based upon the assumption that only the fundamental Floquet mode is important and other modes are negligible. That is, the field variation over a period should be small, or $p \ll \lambda$ (assumption 2). This condition will be automatically satisfied if the frequency of operation is well below the plasma frequency (as discussed in Ref. 27). To illustrate this, rectangular 5×5

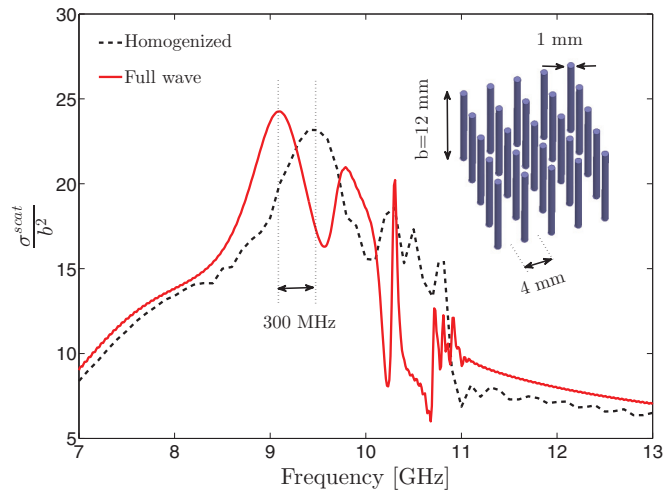

(a) $b = 12$ mm

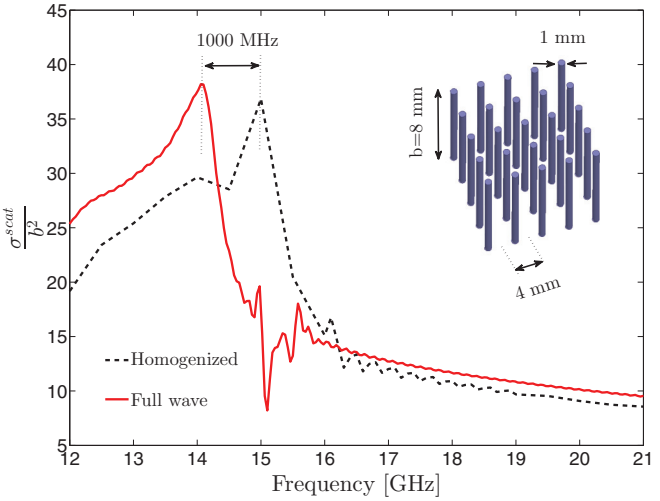

(b) $b = 8$ mm

FIG. 5. (Color online) Normalized scattering cross section of 5×5 wire rectangular objects with $d = 1$ and $p = 4$ mm. For (a) wire length is well longer than the Debye length, whereas for (b) that is not the case, leading to a larger frequency shift between full wave and homogenized results.

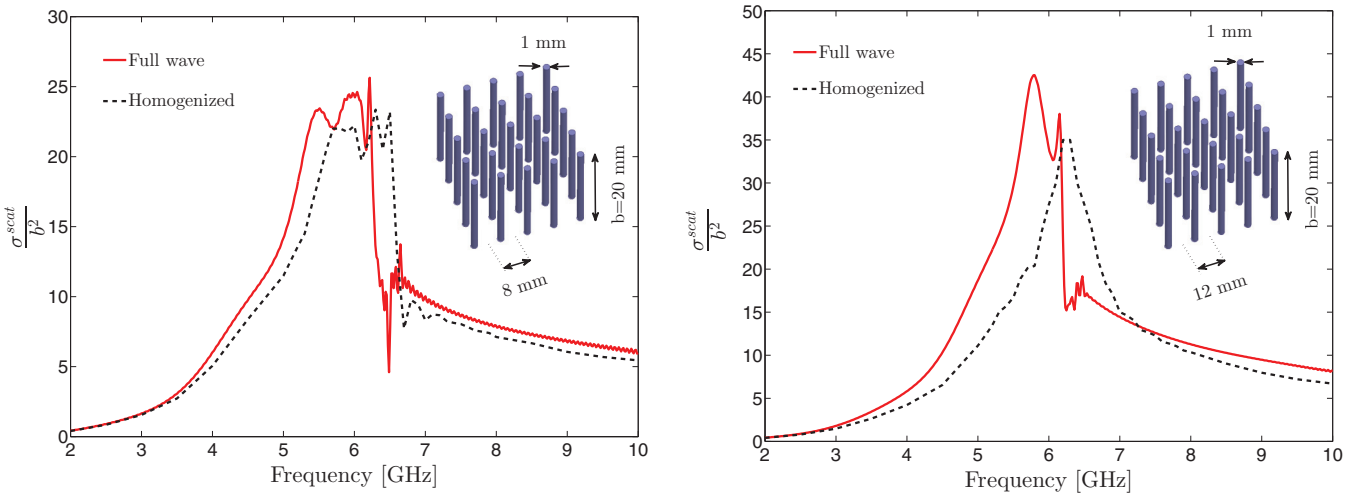

(a) $p = 8$ mm (b) $p = 12$ mm

FIG. 6. (Color online) Normalized scattering cross section of 5×5 wire rectangular objects with $d = 1$ and $b = 20$ mm. The breakdown of homogenization with increasing period is evident.

wire objects are considered with wire diameters of $d = 1$ mm and periods of $p = 4$, 8, and 12, corresponding to plasma frequencies 33.1, 12.3, and 7.3 GHz, respectively. The length of all the wires are chosen to be 20 mm. Figure 6 shows the normalized scattering cross section, comparing full wave and homogenization theory (the $p = 4$ mm results were shown in Fig. 3 and are not repeated here).

The results in Figs. 3 and 6 show that as p increases, the homogenization becomes less accurate. For $p = 8$ mm the homogenization preserves the shape of the curve but shifts the frequency of the scattering. However, for $p = 12$ mm, homogenization in no longer a reasonable approximation since the plasma frequency is lower than the operating frequency. This suggests that when the period is such that the plasma frequency is higher than the frequency of interest, the homogenized model can be used as a reasonable approximation.

Finally, to consider the effect of wire diameters, assumption 1, cubical 5×5 wire objects with $p = 4$ mm and $d =1$, 2, and 3 mm are investigated. Figure 7 shows the normalized scattering cross section for the $d = 2$ and 3 mm cases (the results for $d = 1$ mm were shown in Fig. 3). From Figs. 3 and 7 we conclude that by increasing d, homogenization will have a larger frequency shift in the scattering response from the actual results. However, it still keeps the shape of the curve. This suggests that the homogenization is more sensitive to the period of wires than their thickness. This makes sense because increasing d will increase the plasma frequency (if the period is fixed) and will improve the homogenization approximation. However, the condition $d/p \ll 1$ will be violated and the homogenization becomes worse. Because of these two phenomena acting in apposite directions we can expect that homogenization is less sensitive to wire thickness than to their period.

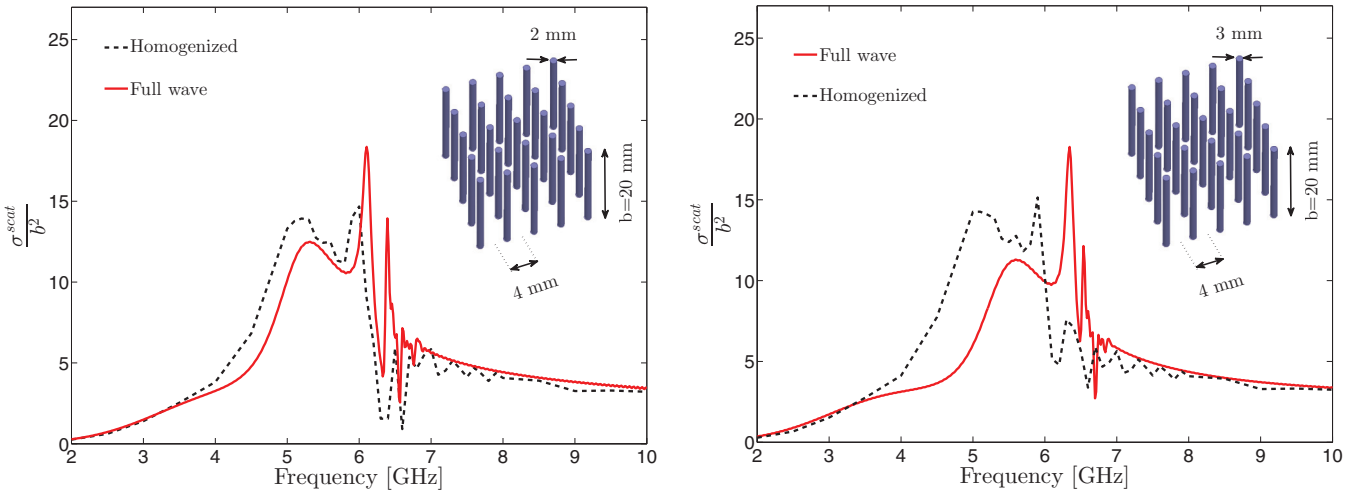

(a) $d = 2$ mm (b) $d = 3$ mm

FIG. 7. (Color online) Normalized scattering cross section of 5×5 wire cubical objects with $p = 4$ mm.

V. CONCLUSION

The interaction of electromagnetic waves and homogenized nonlocal uniaxial wire medium objects were studied using the transport model. The extinction/scattering cross section of several objects was determined and compared to measured and full wave results. The sensitivity of the homogenized model to wire parameters was studied. To have a valid homogenized model for the geometries studied, wire length should be longer than the Debye length. Also, wire diameter and period should be such that the plasma frequency is higher than the operating frequency. The homogenized model is more sensitive to wire period and length that to wire diameter.

*george@uwm.edu

[1] W. Rotman, IRE Trans. Antennas Propag. **10**, 82 (1962).
[2] J. Brown, *Progress in Dielectrics* (Wiley, New York, 1960), pp. 193–225.
[3] D. R. Smith, W. J. Padilla, D. C. Vier, S. C. Nemat-Nasser, and S. Schultz, Phys. Rev. Lett. **84**, 4184 (2000).
[4] P. A. Belov, R. Marques, S. I. Maslovski, I. S. Nefedov, M. Silveirinha, C. R. Simovski, and S. A. Tretyakov, Phys. Rev. B **67**, 113103 (2003).
[5] P. A. Belov and S. A. Tretyakov, J. Electromagn. Waves Appl. **16**, 129 (2002).
[6] X. Zhong, Y. Liu, and K. K. Mei, Microw. Opt. Technol. Lett. **35**, 47 (2002).
[7] T. A. N. Morgado, Ph.D. thesis, University of Coimbra, 2011.
[8] A. N. Rubtsov, M. I. Katsnelson, and A. I. Lichtenstein, Phys. Rev. B **77**, 033101 (2008).
[9] P. A. Belov and M. G. Silveirinha, Phys. Rev. E **73**, 056607 (2006).
[10] M. G. Silveirinha, P. A. Belov, and C. R. Simovski, Phys. Rev. B **75**, 035108 (2007).
[11] C. S. R. Kaipa, A. B. Yakovlev, S. I. Maslovski, and M. G. Silveirinha, Phys. Rev. B **86**, 155103 (2012).
[12] P. A. Belov, Y. Hao, and S. Sudhakaran, Phys. Rev. **73**, 033108 (2006).
[13] P. A. Belov, Y. Zhao, S. Tse, P. Ikonen, M. G. Silveirinha, C. R. Simovski, S. Tretyakov, Y. Hao, and C. Parini, Phys. Rev. B **77**, 193108 (2008).
[14] P. A. Belov, Y. Zhao, S. Sudhakaran, A. Alomainy, and Y. Hao, Appl. Phys. Lett. **89**, 262109 (2006).
[15] A. Rahman, P. A. Belov, M. G. Silveirinha, C. R. Simovski, Y. Hao, and C. Parini, Appl. Phys. Lett. **94**, 031104 (2009).
[16] P. A. Belov, G. K. Palikaras, Y. Zhao, A. Rahman, C. R. Simovski, Y. Hao, and C. Parini, Appl. Phys. Lett. **97**, 191905 (2010).
[17] M. G. Silveirinha, P. A. Belov, and C. R. Simovski, Opt. Lett. **33**, 1726 (2008).
[18] P. A. Belov, Y. Zhao, Y. Hao, and C. Parini, Opt. Lett. **34**, 527 (2009).
[19] I. Nefedov, D. Chicherin, and A. Viitanen, *Proceedings of SPIE*, Metamaterials III (SPIE, Bellingham, WA, 2008), Vols. 69 and 87, pp. 698–728.
[20] G. Lovat, P. Burghignoli, and S. Celozzi, IEEE Trans. Electromag. Comp. **50**, 80 (2008).
[21] S. Hrabar, *Metamaterials and Plasmonics: Fundamentals, Modeling, Applications*, NATO Science for Peace and Security Series B: Physics and Biophysics (Springer, New York, 2009), Part IV, pp. 139–151.
[22] P. Burghignoli, G. Lovat, F. Capolino, V. Jackson, and D. Wilton, IEEE Trans. Antennas Propag. **56**, 1329 (2008).
[23] C. R. Simovski, P. A. Belov, A. V. Atrashchenko, and Y. S. Kivshar, Adv. Mater. **24**, 4229 (2012).
[24] A. L. Pokrovsky and A. L. Efros, Phys. Rev. Lett. **89**, 093901 (2002).
[25] A. L. Pokrovsky and A. L. Efros, Phys. Rev. B **65**, 045110 (2002).
[26] A. L. Pokrovsky, Phys. Rev. B **69**, 195108 (2004).
[27] M. G. Silveirinha, Phys. Rev. E **73**, 046612 (2006).
[28] F. Lemoult, G. Lerosey, J. de Rosny, and M. Fink, Phys. Rev. Lett. **104**, 203901 (2010).
[29] F. Lemoult, M. Fink, and G. Lerosey, Waves in Random and Complex Media **21**, 591 (2011).
[30] F. Lemoult, M. Fink, and G. Lerosey, Nat. Commun. **3**, 889 (2012).
[31] F. Lemoult, N. Kaina, M. Fink, and G. Lerosey, Nat. Phys. **9**, 55 (2013).
[32] CST Microwace Studio, http://www.CST.com.
[33] Y. Zhao, P. A. Belov, and Y. Hao, Opt. Express **14**, 5154 (2006).
[34] K. M. Yassien, J. Opt. A: Pure Appl. Opt. **11**, 075701 (2009).
[35] Y. Zhao, P. A. Belov, and Y. Hao, IEEE Trans. Antennas Propag. **55**, 1506 (2007).
[36] M. Hudlika, J. Machac, and I. S. Nefedov, PIER **65**, 233 (2006).
[37] W. Chew, *Waves and Fields in Inhomogeneous Media* (IEEE, New York, 1995).
[38] P. Halevi, *Spatial Dispersion in Solids and Plasmas* (North Holland, Amsterdam, 1992).
[39] G. Hanson, M. Silveirinha, P. Burghignoli, and A. Yakovlev, New J. Phys. **15**, 083018 (2013).
[40] E. Forati and G. Hanson [Appl. Phys. Lett. (to be published)].
[41] M. G. Silveirinha, Phys. Rev. B **79**, 035118 (2009).
[42] G. W. Hanson, E. Forati, and M. G. Silveirinha, IEEE Trans. Antennas Propag. **60**, 4219 (2012).
[43] E. Forati and G. W. Hanson, IEEE Trans. Antennas Propag. **61**, 3564 (2013).
[44] A. D. Yaghjian, Proc. IEEE **68**, 248 (1980).
[45] M. Silveirinha, IEEE Trans. Antennas Propag. **54**, 1766 (2006).
[46] R. Newton, Am. J. Physics **44**, 639 (1976).
[47] QWED Inc., Warsaw, Poland, www.qwed.com.pl.
[48] Structure Probe Inc., SPI Flash-Dry Silver Paint.